Journal of Thrombosis and Haemostasis, **16**: 303–315 DOI: 10.1111/jth.13917

ORIGINAL ARTICLE

Identification of aggregates in therapeutic formulations of recombinant full-length factor VIII products by sedimentation velocity analytical ultracentrifugation

J. F. HEALEY, E. T. PARKER and P. LOLLAR
Department of Pediatrics, Aflac Cancer and Blood Disorders Center, Children's Healthcare of Atlanta, Emory University, Atlanta, GA, USA

To cite this article: Healey JF, Parker ET, Lollar P. Identification of aggregates in therapeutic formulations of recombinant full-length factor VIII products by sedimentation velocity analytical ultracentrifugation. *J Thromb Haemost* 2018; **16**: 303–15.

Essentials

- Factor VIII inhibitors are the most serious complication in patients with hemophilia A.
- Aggregates in biopharmaceutical products are an immunogenic risk factor.
- Aggregates were identified in recombinant full-length factor VIII products.
- Aggregates in recombinant factor VIII products are identified by analytical ultracentrifugation.

Summary. *Background:* The development of inhibitory anti-factor VIII antibodies is the most serious complication in the management of patients with hemophilia A. Studies have suggested that recombinant full-length FVIII is more immunogenic than plasma-derived FVIII, and that, among recombinant FVIII products, Kogenate is more immunogenic than Advate. Aggregates in biopharmaceutical products are considered a risk factor for the development of anti-drug antibodies. *Objective:* To evaluate recombinant full-length FVIII products for the presence of aggregates. *Methods:* Advate, Helixate and Kogenate were reconstituted to their therapeutic formulations, and subjected to sedimentation velocity (SV) analytical ultracentrifugation (AUC). Additionally, Advate and Kogenate were concentrated and subjected to buffer exchange by ultrafiltration to remove viscous cosolvents for the purpose of measuring $s_{20,w}$ values and molecular weights. *Results:* The major component of all three products was a population of ~7.5 S heterodimers with a weight-average molecular weight of ~230 kDa. Helixate and Kogenate contained aggregates ranging from 12 S to at least 100 S, representing ≈ 20% of the protein mass. Aggregates greater than 12 S represented < 3% of the protein mass in Advate. An approximately 10.5 S aggregate, possibly representing a dimer of heterodimers, was identified in buffer-exchanged Advate and Kogenate. SV AUC analysis of a plasma-derived FVIII product was confounded by the presence of von Willebrand factor in molar excess over FVIII. *Conclusions:* Aggregate formation has been identified in recombinant full-length FVIII products, and is more extensive in Helixate and Kogenate than in Advate. SV AUC is an important method for characterizing FVIII products.

Keywords: aggregates; analytical ultracentrifugation; factor VIII; hemophilia A; immunogenicity.

Correspondence: Pete Lollar, Room 438, Emory Children's Center, Emory University, 2015 Uppergate Drive, Atlanta, GA 30322, USA
Tel.: +1 404 727 5569
E-mail: jlollar@emory.edu

Received: 26 April 2017
Manuscript handled by: D. DiMichele
Final decision: P. H. Reitsma, 19 November 2017

Introduction

The most serious complication in the management of patients with hemophilia A is the development of inhibitory anti-factor VIII antibodies (inhibitors). Inhibitors occur in 30–40% of previously untreated children with hemophilia A following initiation of FVIII replacement therapy [1–4]. Patient-related risk factors for inhibitor development include poorly understood genetic and non-genetic factors [5,6]. Observational studies have indicated that recombinant products are more immunogenic than plasma-derived products [7–9], although this has not been confirmed by other studies [4,10–13]. The randomized SIPPET trial found that patients treated with plasma-derived FVIII containing von Willebrand factor (VWF) had a lower incidence of inhibitors than those treated with recombinant FVIII [14]. The differential immunogenicity was higher in patients with a relatively low risk of inhibitor development because of non-null mutations in the *F8* gene [15]. Additionally, observational studies have indicated that, among the recombinant full-length FVIII products, Kogenate and Helixate are more

immunogenic than Advate [4,16,17]. The problems associated with interpreting these studies have been discussed extensively [18–20].

Protein aggregates in biopharmaceuticals constitute a risk factor for the development of anti-drug antibodies [21]. Aggregation is defined as self-association of a protein to form stable covalent or non-covalent complexes. Sedimentation velocity (SV) analytical ultracentrifugation (AUC) has emerged as a powerful method for detecting protein aggregates in biopharmaceuticals [22]. In contrast to size exclusion chromatography (SEC), gel electrophoresis, and other fractionation-dependent techniques, SV AUC is a matrix-free method that does not disturb the self-association process, and provides size and conformation information about the protein and its aggregates. Additionally, analysis can be performed in the product formulation buffer. The most widely used method for measuring protein aggregates by SV AUC is $c(s)$ distribution analysis with the program SEDFIT [23,24]. This method produces an estimate of the distribution of sedimentation coefficients within a heterogeneous population of proteins, buffer components, and excipients. Additionally, it provides an estimate of the mass of aggregates present in a protein product.

In this study, we reconstituted Advate, Helixate and Kogenate into their injectable formulations, and subjected the products to SV AUC. We identified aggregates extending up to 100 S in Helixate and Kogenate. Additionally, in all three products, we identified a 10.5 S aggregate that represents a dimer of FVIII heterodimers.

Materials and methods

Materials

Advate (Baxter, Westlake Village, CA, USA), Helixate FS (CSL Behring, Kankakee, IL, USA) and Kogenate FS (Bayer Corporation, Whippany, NJ, USA) were purchased from their respective manufacturers. Manufacturing lots and product characteristics are described in Tables S1 and S2. Formulated products were prepared by adding Sterile Water for Injection by use of the kits and instructions provided by the manufacturers. These formulations represent the products as they would be administered to a patient. FVIII activity measured with a one-stage clotting assay [25] yielded values within the experimental error of the nominal values in Table S1. Advate, Helixate and Kogenate also were concentrated 4.6-fold and subjected to buffer exchange by repeated filtration with an Amicon Ultra-15 Ultracel-30K centrifugal filter. After passivation of the filter with 0.15 M NaCl, 0.02 M HEPES and 5 mM $CaCl_2$ (HBS/Ca^{2+}) with 0.01% polysorbate 80 (pH 7.4), 1.5-mL samples were filtered by centrifugation at 2400 × *g* at 4 °C to ~ 0.05 mL; this was followed by the addition of 3.9 mL of HBS/Ca^{2+}, and further concentration to ~ 0.05 mL. After the centrifugation/filtration step had been repeated three times, the sample was collected in 0.33 mL of HBS/Ca^{2+}.

Wilate (870 IU of VWF ristocetin cofactor activity per vial; 940 IU of FVIII per vial) was purchased from Octapharma (Vienna, Austria), and reconstituted to its therapeutic formulation by adding Sterile Water for Injection. Human plasma-derived VWF was purified as described previously [26]. Polysorbate 80 (10% Tween-80 Surfact-Amps Detergent Solution) was purchased from Thermo Scientific (Waltham, MA, USA). Anotop 10 0.02-μm syringe filters were purchased from Sigma Aldrich (St Louis, MO, USA). Amicon Ultra-15 Ultracel-30K centrifugal filters were purchased from Merck Millipore (Billerica, MA, USA).

UV absorbance spectroscopy

UV absorbance scans of formulated Advate, Helixate and Kogenate and of polysorbate 80 were performed in a Beckman DU650 spectrophotometer (Indianapolis, IN, USA) in a 1-cm-pathlength quartz cell blanked against water.

AUC

SV experiments were performed at 105 000 × *g* on Advate, Helixate, Kogenate, and Wilate, or at 42 000 × *g* on purified VWF at 20 °C in a Beckman Coulter ProteomeLab XLI analytical ultracentrifuge. Scanning was performed at 280 nm in an An-60 rotor equipped with 12-mm-pathlength double-sector cells and sapphire windows. For formulated Advate, Helixate, Kogenate, Wilate, and VWF, water was used in the reference sector. For buffer-exchanged samples, ultrafiltration buffer was used in the reference sector. Sample and reference buffer volumes were 0.40 mL each. Scans were initiated in continuous mode with a radial spacing of 0.003 cm after reaching the target rotor speed, and were acquired at intervals of ≈ 3 min.

Data were analyzed with SEDFIT, version 15.01c (http://analyticalultracentrifugation.com) by use of the continuous $c(s)$ distribution model [23,27]. This model produces a least squares fit of the absorbance signal as a function of radial position and time to a set of Lamm equations corresponding to a user-defined range and increments of sedimentation coefficients. The meniscus position, baseline and time-invariant noise were also fitted. Fitting was performed by maximum entropy regularization with a confidence interval of 0.68. Both the simplex and Marquardt–Levenberg non-linear least squares fitting algorithms were tested, and produced equivalent results.

Molecular weight estimates were obtained for the dominant species in buffer-exchanged Advate and Kogenate from the Svedberg equation by deconvoluting the contribution of diffusion to the observed signal as described previously [23,28]. The sedimentation coefficients ($s_{20,w}$ values) of buffer-exchanged Advate and Kogenate were converted to the standard condition of water as reference

solvent at 20 °C as described by Svedberg and Pedersen [29]. The viscosity and density of the exchange buffer used in the determination were estimated with SEDNTERP (http://sednterp.unh.edu) [30]. SV graphs were plotted with GUSSI version 1.2.1 [31].

Weight-average molecular weight and partial specific volume of full-length FVIII

The weight-average molecular weight and partial specific volume of full-length FVIII were estimated from the fractional distribution of FVIII heterodimers and their glycan contents following integration of SEC peaks of fractionated FVIII light chain (LC) and heavy chain (HC) species 1–817, 1–1115, and 1–1313 [32]. The mole fraction of each species, f_i, was estimated by the use of molar extinction coefficients predicted from their tryptophan, tyrosine and cystine contents [33], with

$$f_i = \frac{F_i / \varepsilon_{HC_i}}{\sum_{i=1}^{3} F_i / \varepsilon_{HC_i}}$$

where F_i and ε_i are the signal of the integrated SEC peak and the extinction coefficient of HC species i, respectively.

The A1 domain and LC each have two N-linked glycans [34]. In the B domain, there are 14 occupied N-linked glycan sites between residues 741 and 1313 [34], yielding two, nine and 14 N-linked glycans for the $HC_{1–817}$, $HC_{1–1115}$ and $HC_{1–1313}$ species, respectively. Most of the N-linked glycans in full-length FVIII are (i) disialo, core-fucosylated biantennary, (ii) monosialo, core-fucosylated biantennary and (iii) trisialo core-fucosylated triantennary glycans at a weight ratio of approximately 2.2 : 1 : 1 [35]. This ratio produces a weight-average glycan mass of 2439 Da. The glycan mass obtained by multiplying the number of N-linked glycans by weight-average mass was added to the polypeptide mass to estimate the molecular weight of each heterodimer.

The weight fraction of species i is given by

$$w_i = \frac{f_i M_i}{\sum_{i=1}^{3} f_i M_i}$$

where M_i is the molecular weight and f_i is the mole fraction. The weight-average molecular weight is

$$M_w = \sum_{i=1}^{3} w_i M_i$$

Using the estimates of f_i and M_i yielded a weight-average molecular weight for full-length FVIII of 246 kDa.

The partial specific volume, $\bar{v}$, of a glycoprotein was estimated by using

$$\bar{v} = w_{\text{polypeptide}} \bar{v}_{\text{polypeptide}} + w_{\text{glycan}} \bar{v}_{\text{glycan}}$$

where $w_{\text{polypeptide}}$ and w_{glycan} and $\bar{v}_{\text{polypeptide}}$ and $\bar{v}_{\text{glycan}}$ are the weight fractions and partial specific volumes of the polypeptide and glycan. The partial specific volumes of the $HC_{1–817}$–LC, $HC_{1–1115}$–LC and $HC_{1–1313}$–LC heterodimers estimated with SEDNTERP are, identically, 0.733 mL g^{-1}. A partial specific volume of glycoprotein glycans of 0.63 mL g^{-1} was used [36]. With these values and the fractional glycan content of the FVIII heterodimers, a weight-average partial specific volume of 0.719 mL g^{-1} was obtained for full-length FVIII.

SEC

SEC was performed on 0.1-mL samples with a Superdex 200 Increase 10/300GL column (GE Healthcare Life Sciences, Marlborough, MA, USA) at 0.75 mL min^{-1}, with 0.4 M NaCl, 0.025 M HEPES, 5 mM $CaCl_2$ and 0.01% Tween-80 (pH 7.4) as the running buffer, and absorbance at 280 nm for detection. Advate (Lot 2) and Kogenate (Lot 3) were reconstituted to their therapeutic formulations and injected without further manipulation.

Results

UV absorbance spectra of formulated Advate, Helixate, and Kogenate

Advate, Helixate and Kogenate were reconstituted with Sterile Water for Injection by use of the kits supplied by the manufacturers, producing the formulation used for therapeutic, intravenous delivery. SDS-PAGE analysis of the preparations revealed major bands at approximately 200 kDa and 80 kDa corresponding to the FVIII HC and LC, and thrombin activation fragments at approximately 75, 50 and 40 kDa corresponding to the thrombin-activated light chain and A1 and A2 subunits of activated FVIII, as previously described [32] (Fig. S1). In anticipation of using absorbance at 280 nm to detect the properties of Advate, Helixate and Kogenate in the analytical ultracentrifuge, UV absorbance spectra of the formulated products were obtained (Fig. 1). The spectra revealed characteristic protein absorbance peaks at 278 nm attributable to tryptophan and tyrosine, and a shoulder at 288 nm attributable to tryptophan. Polysorbate 80 is present as a stabilizer in Lot 1 and Lot 2 of Advate at concentrations of 0.3 mg mL^{-1} and 0.1 mg mL^{-1}, respectively, and at ~0.08 mg mL^{-1} in Helixate and Kogenate (Table S2). The UV absorbance spectrum of a 1 mg mL^{-1} solution of polysorbate 80 produces an OD resulting from combined absorbance and light scattering of 0.05 at 280 nm (Fig. S2), consistent with published results [37]. This indicates that polysorbate 80 makes a minor contribution to the absorbance at 280 nm at the concentrations present in the formulated products. The formulations also possessed significant turbidity resulting from light scattering, as shown by the non-zero OD between 310 nm and 340 nm.

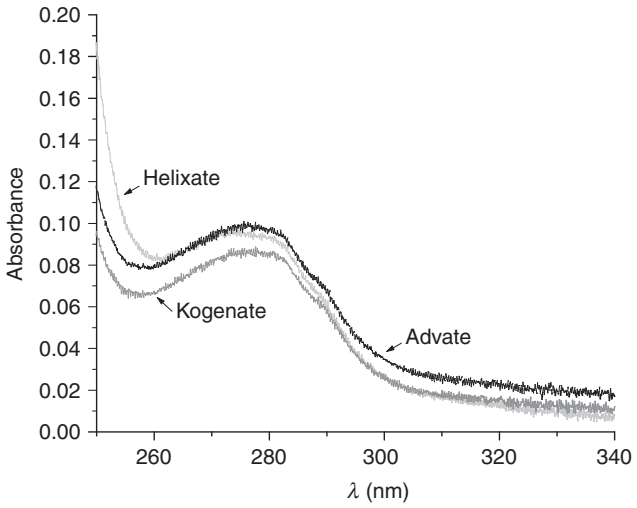

Fig. 1. UV absorbance spectra of full-length FVIII products. Lyophilized vials of Advate, Helixate and Kogenate were reconstituted in Sterile Water for Injection to produce their therapeutic formulations, and absorbance spectra were obtained at 0.1-nm intervals in a 1-cm-pathlength cuvette blanked against water. Light gray: Helixate. Gray: Kogenate. Black: Advate.

SV analysis of formulated Advate

Two lots of Advate were reconstituted to their therapeutic formulations and immediately subjected to SV AUC. Figure 2A,C shows overlays of scans of $A_{280\ nm}$ versus radial position taken at different times during the sedimentation process. The scans were fitted to the continuous $c(s)$ distribution model in SEDFIT. The least squares fits are shown in Fig. 2A,C, and the resulting $c(s)$ distributions are shown in Fig. 2B,D. The non-zero baselines in Fig. 2A,C are attributable to presence of a 0.2-S solvent species. In Lot 1, a major $c(s)$ peak was present at 4.6 S, preceded by a small shoulder (Fig. 2B). In Lot 2, there was a major 6.7 S peak, there were minor peaks at 4.3 S and 10.2 S, and there was a broad distribution between 12 S and 20 S (Fig. 2D). Excluding the solvent peak (not shown), the 6.7 S, 4.3 S, 10.2 S and 12–20-S distributions represent 81%, 6.9%, 5.5% and 3.8% of the $A_{280\ nm}$ signal, respectively.

The difference in sedimentation coefficients of the major species in Lot 1 and Lot 2 is the result of differences in the stabilizers and excipients in the formulated products. The lots had the same components, but they were present at a 2.4-fold higher concentration in Lot 1 than in Lot 2 (Table S2). An increase in solution viscosity and density associated with higher cosolvent concentrations slows particle transport, and therefore reduces the sedimentation coefficient.

SV analysis of formulated Helixate and Kogenate

Helixate Lot 1 and Kogenate Lot 1 were reconstituted in Sterile Water for Injection and immediately subjected to SV AUC. Figure 3A,C shows an overlay of the absorbance scans and least squares fits to a continuous $c(s)$ distribution. Figure 3B,D shows the resulting $c(s)$ distributions. Both products gave a broad peak below 20 S. In contrast to Advate, species of up 100 S were detected in both products. Integration of the $c(s)$ distributions from two lots of each product yielded estimates of the amounts of materials migrating between 12 S and 20 S and between 20 S and 100 S (Fig. 4). Approximately 20% of the mass in Helixate and Kogenate is attributable to aggregates with sedimentation coefficients between 12 S and 100 S. SV AUC was also performed on formulated Helixate and Kogenate samples passed through a 0.02-μm filter, which did not decrease the fraction of 12–100 S aggregates (data not shown).

SV analysis of heat-treated Advate and Kogenate

In a modification of the Nijmegen–Bethesda FVIII inhibitor assay, samples are heated at 56 °C for 30 min, which inactivates FVIII but does not destroy the inhibitor [38]. Heat denaturation of Advate and Kogenate under these conditions resulted in near-complete aggregation to products sedimenting at 20–100 S (Fig. S3).

SEC of Advate and Kogenate

Advate and Kogenate were reconstituted to their therapeutic formulations and subjected to SEC for comparison with the results obtained with SV AUC (Fig. 5). Both products yielded peaks that eluted slightly ahead of the 670-kDa thyroglobulin standard, consistent with an anomalously high apparent molecular weight resulting from particle asymmetry. There were no obvious aggregates identified in the chromatograms. Peak height recovery was evaluated with IgG mAb 2-76 as a standard. mAb 2-76 produced a linear relationship between peak height $A_{280\ nm}$ and injected $A_{280\ nm}$. The slope of the line, 0.27, representing the ratio of peak height/injected $A_{280\ nm}$, is a result of sample dilution during the run. The injected $A_{280\ nm}$ and peak height $A_{280\ nm}$ for Advate were 10.2 and 1.1, respectively, and those for Kogenate were 5.6 and 0.7, respectively. The corresponding ratios of peak height/injected $A_{280\ nm}$ values for Advate and Kogenate were 0.11 and 0.13. These values are lower than the ratio for mAb 2-76, indicating adsorptive losses of Advate and Kogenate. Overall, the results are consistent with the inability of SEC to detect aggregates in Advate and Kogenate, because of a decrease in signal/noise ratio resulting from sample dilution and adsorptive losses to the chromatography matrix.

SV analysis of buffer-exchanged, concentrated Advate and Kogenate

The molecular weights of the major species in Advate and Kogenate were estimated by SV AUC to determine

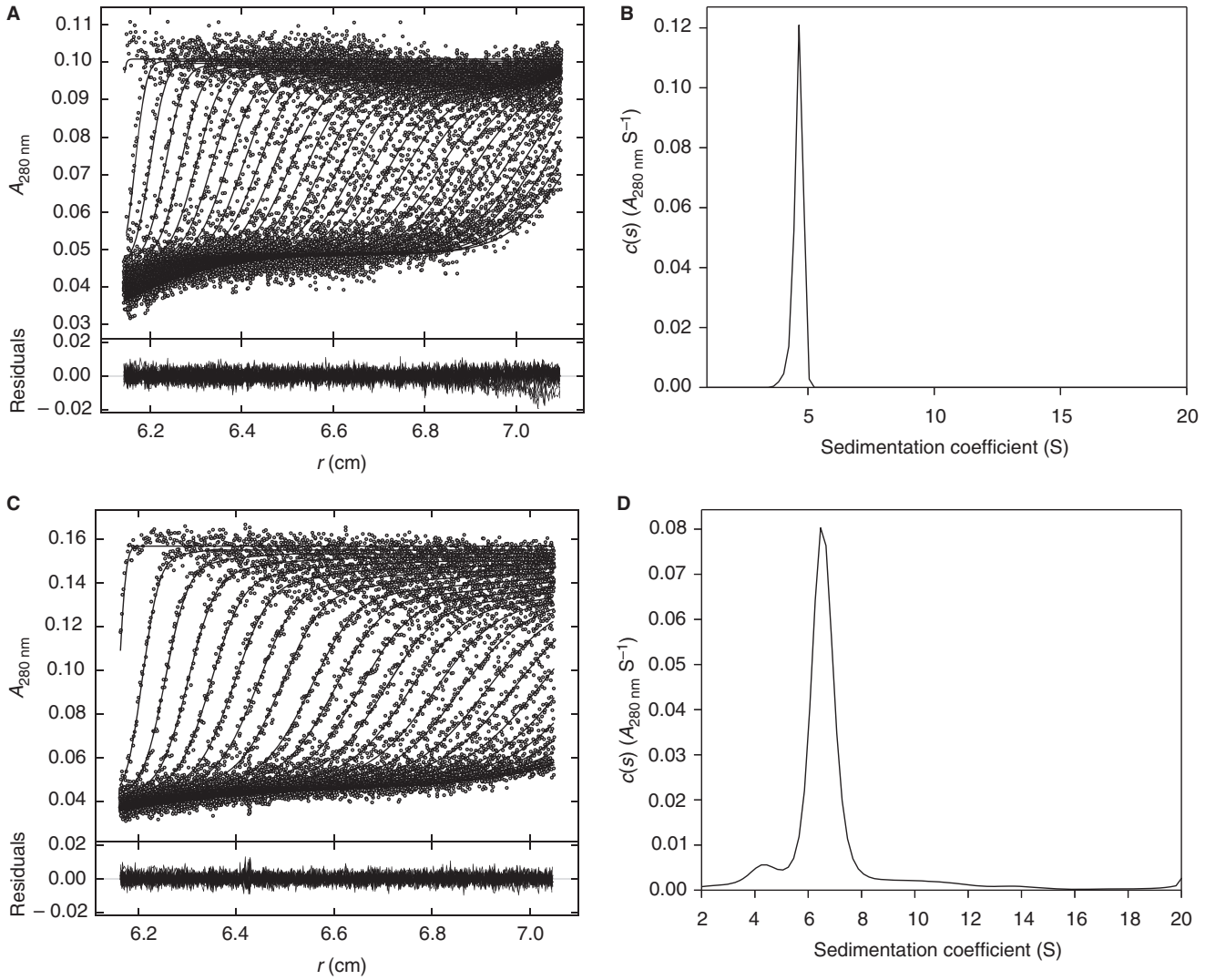

Fig. 2. Sedimentation velocity (SV) analytical ultracentrifugation (AUC) of formulated Advate. Lyophilized vials of Advate, Lot 1 (A, B) and Lot 2 (C, D) were reconstituted in Sterile Water for Injection to produce their therapeutic formulations, and then subjected to SV AUC at 105 000 × *g* at 20 °C. (A, C) $A_{280\ nm}$ scans were taken at 3-min intervals, and fitted to a continuous *c*(*s*) distribution from 0 S to 20 S with 0.2-S increments. Only every fourth scan is shown for clarity. The lower panels show the residuals of the fitted data. The root-mean-square deviations of the fits are 0.0032 and 0.0027, respectively. (B, D) *c*(*s*) distributions. Solvent peaks at 0.2 S are not shown.

whether they represent heterodimeric FVIII or aggregates. To eliminate potential cosolvent effects of stabilizers and excipients, Lot 1 of formulated Advate and Lot 1 of formulated Kogenate were exchanged into HBS/Ca^{2+} (pH 7.4), and concentrated 4.6-fold by repeated ultrafiltration with a 30-kDa-cutoff membrane. Figure 6A,C shows the resulting $A_{280\ nm}$ scans and least squares fits to continuous *c*(*s*) distributions. The increase in concentration increased the signal/noise ratio, improving the resolution in the *c*(*s*) distributions shown in Fig. 6B,D as compared with Fig. 2B,D and Fig. 3D. Additionally, buffer exchange allowed measurement of standard $s_{20,w}$ values. Both products showed a dominant peak at 7.4–7.5 S and additional peaks at 5.0–5.1 S and 10.5–10.6 S (Fig. 6B,D). There were additional species in Kogenate in the 20–100-S range, as in the formulated product prior to buffer exchange (data not shown).

Continuous *c*(*s*) analysis in SEDFIT provides an estimate of a weight-average frictional ratio, f/f_0, which, when combined with the $s_{20,w}$ value and the partial specific volume, provides a molecular weight estimate of the sedimenting species [23,39]. These estimates are valid when the sample is monodisperse or when the frictional ratios of all of the sedimenting species are equal [23]. The frictional ratios obtained for Advate and Kogenate were 1.82 and 1.91, respectively, producing molecular weight estimates of 220 kDa and 230 kDa, respectively (Table 1). These values can be compared with a weight-average molecular weight of 246 kDa for full-length FVIII based on estimates of the weight fraction of the HCs [32] and

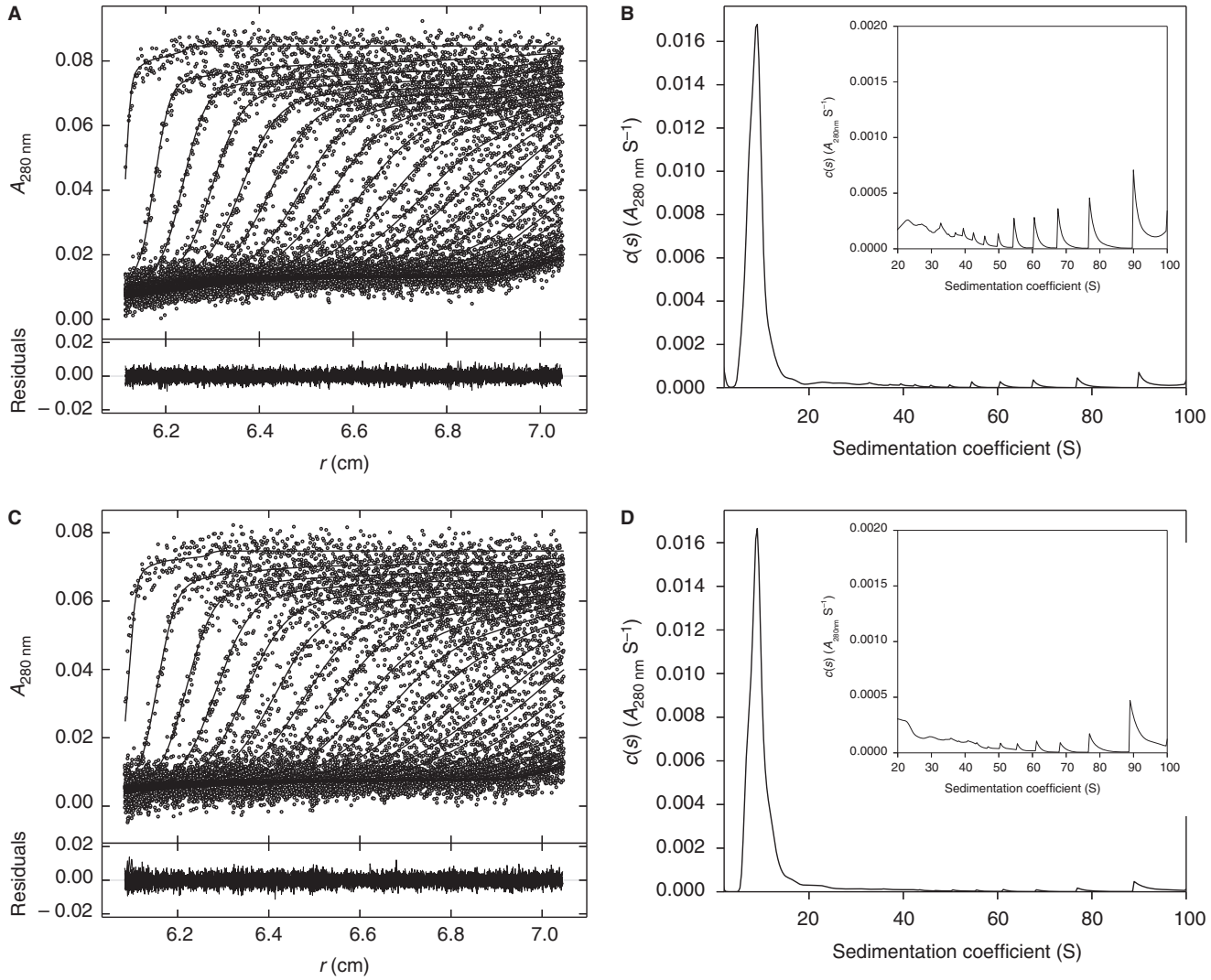

Fig. 3. Sedimentation velocity (SV) analytical ultracentrifugation (AUC) of formulated Helixate and Kogenate. Lyophilized vials of Helixate Lot 2 (A, B) and Kogenate Lot 2 (C, D) were reconstituted in Sterile Water for Injection to produce their therapeutic formulations, and then subjected to SV AUC at 105 000 × *g* at 20 °C. (A, C) $A_{280\ nm}$ scans were taken at approximately 3-min intervals, and fitted to a continuous *c* (*s*) distribution from 0 S to 100 S with 0.3-S increments. Only every fourth scan is shown for clarity. The root-mean-square deviations of the fits are 0.0024 and 0.0027, respectively. The lower panels show the residuals of the fitted data. (B, D) *c*(*s*) distributions. Insets: expanded scale. Solvent peaks at 0.2 S are not shown.

the mass contribution made by N-linked glycans [34,35], as described in Materials and methods (Table 2). This calculation slightly overestimates the weight-average molecular weight because a minor but unknown fraction of the sites containing N-linked glycans is unoccupied [34]. Thus, the results are consistent with a 7.5 S heterodimer being the dominant species present in Advate and Kogenate.

Polysorbate 80 micelles have a reported molecular weight of ≈ 120 kDa [40]. Thus, the micelles are retained and are coconcentrated during ultrafiltration with a 30-kDa-cutoff membrane. This resulted in estimated concentrations of polysorbate 80 of 1.4 mg mL^{-1} and 0.4 mg mL^{-1} in Advate and Kogenate, respectively, based on their nominal concentrations prior to concentration (Table S2). The peaks at 1.6–1.7 S in Fig. 5B,D are attributable to polysorbate 80, which was verified by SV analysis of polysorbate 80 subjected to the same ultrafiltration procedure in the absence of FVIII (data not shown).

SV analysis of a commercial plasma-derived FVIII product

Although the focus of the current study was to compare full-length recombinant FVIII products, in initial studies we examined the SV properties of the plasma-derived FVIII product Wilate (Fig. 7A,B). For comparison, fitted absorbance scans and the continuous *c*(*s*) distribution for highly purified plasma-derived human VWF are shown (Fig. 7C,D). Wilate and purified VWF showed peaks at

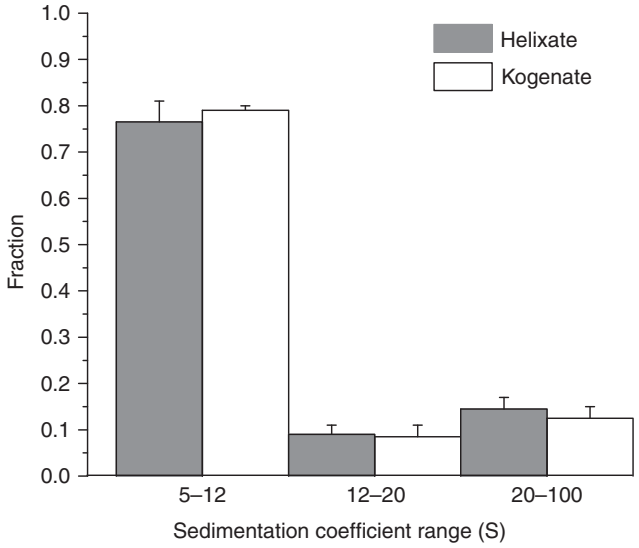

Fig. 4. Distribution of sedimentation coefficients in Helixate and Kogenate. *c*(*s*) distributions resulting from sedimentation velocity analytical ultracentrifugation of two lots each of formulated of Helixate and Kogenate were integrated between 5 S and 12 S, 12 S and 20 S, and 20 S and 100 S, and normalized to the integration between 5 S and 100 S. Shown are means and ranges of the two determinations.

~ 20 S and 30 S, respectively.The lower sedimentation coefficient in the Wilate peak is attributable, at least in part, to increased solvent viscosity resulting from the presence of sucrose as a stabilizer (Table S2). Material sedimenting in the 40–100-S range constituted 4% and 6% of the total signals of Wilate and purified VWF, respectively.

Discussion

In this article, we report the identification of aggregates in recombinant full-length FVIII products by the use of SV AUC. The presence of aggregates in a biopharmaceutical product is considered an immunogenic risk [41]. Current Food and Drug Administration guidance states that 'it is critical for manufacturers of therapeutic protein products to minimize protein aggregation to the extent possible' [42]. The immunogenicity of protein aggregates has been studied extensively for > 50 years [43]. Aggregates have been implicated in the immunogenicity of intravenous immunoglobulin [44], human growth hormone [45], interferon-α [46], and other biopharmaceuticals, including plasma-derived FVIII [47]. The mechanisms by which aggregates increase immunogenicity are not well understood, and may be specific to the product. Studies in model systems have indicated that aggregates can activate both the adaptive immune system and the innate immune system. The presence of two or more epitopes in an aggregate can cross-link the B-cell receptor, leading to B-cell proliferation and antigen presentation [41,48,49]. Partial unfolding of a protein can produce aggregates through interactions between exposed hydrophobic surfaces. It has been proposed that residual hydrophobic patches on aggregates form damage-associated molecular patterns that activate innate immunity [50].

Lyophilized preparations of Advate, Helixate and Kogenate reconstituted to their therapeutic formulations contain sufficient absorbance at 280 nm for the sedimentation properties of the product components, including aggregates, to be determined (Figs 2 and 3). Approximately 20% of the mass in Helixate and Kogenate was attributable to aggregates with sedimentation coefficients ranging from 12 S up to at least 100 S (Fig. 4). Helixate and Kogenate showed indistinguishable sedimentation behavior, as expected because they are the same product sold under different labels. Although Helixate and Kogenate originate from the same manufacturing process through fill-and-finish, post-manufacture product storage and handling potentially affect the immunogenicity of therapeutic proteins [51]. In the absence of knowledge in the public domain about differences in post-manufacture product storage and handling between Helixate and Kogenate, we treated them as separate products. In contrast, aggregates exceeding 20 S were not identified in Advate. Advate Lot 2 contained 4% of aggregates between 12 S and 20 S. No aggregates in this range were identified in Lot 1 Advate. The immunogenicity of protein aggregates increases with size in some experimental systems [52–54]. Thus, the presence of large aggregates in Helixate and Kogenate may contribute to the increased incidence of FVIII inhibitor formation as compared with Advate that has been suggested by some studies [4,16,17]. There were no differences in the size and amount of aggregates in Helixate and Kogenate products whose storage ranged over several years (Fig. 4; Table S1), indicating that aggregates are formed during the manufacturing process and are stable thereafter. This may occur during manufacturing fill-and-finish with its attendant alteration of the aqueous milieu of the FVIII protein.

All three products employ sugars as stabilizers. Lot 1 of formulated Advate contained 0.44 M mannitol, and at least two-fold increased concentrations of all excipients and stabilizers as compared with Lot 2. Submolar concentrations of sugars and other cosolvents have large effects on the sedimentation properties of molecules [55–58]. This was evident on comparison of Lot 1 and Lot 2 of Advate, in which the sediment coefficients of the major species were 4.6 S and 6.7 S, respectively. Buffer exchange and concentration of Advate and Kogenate were performed to reduce cosolvent effects and to increase the signal/noise ratio. This led to the identification of a 10.5–10.6 S peak in Advate and Kogenate, representing 7% and 5% of the protein-related absorbance signal, respectively (Fig. 6B,D). According to the $s \sim M^{2/3}$ power law relationship between molecular weight and the sedimentation coefficient [59], the ~ 10.5 S species is

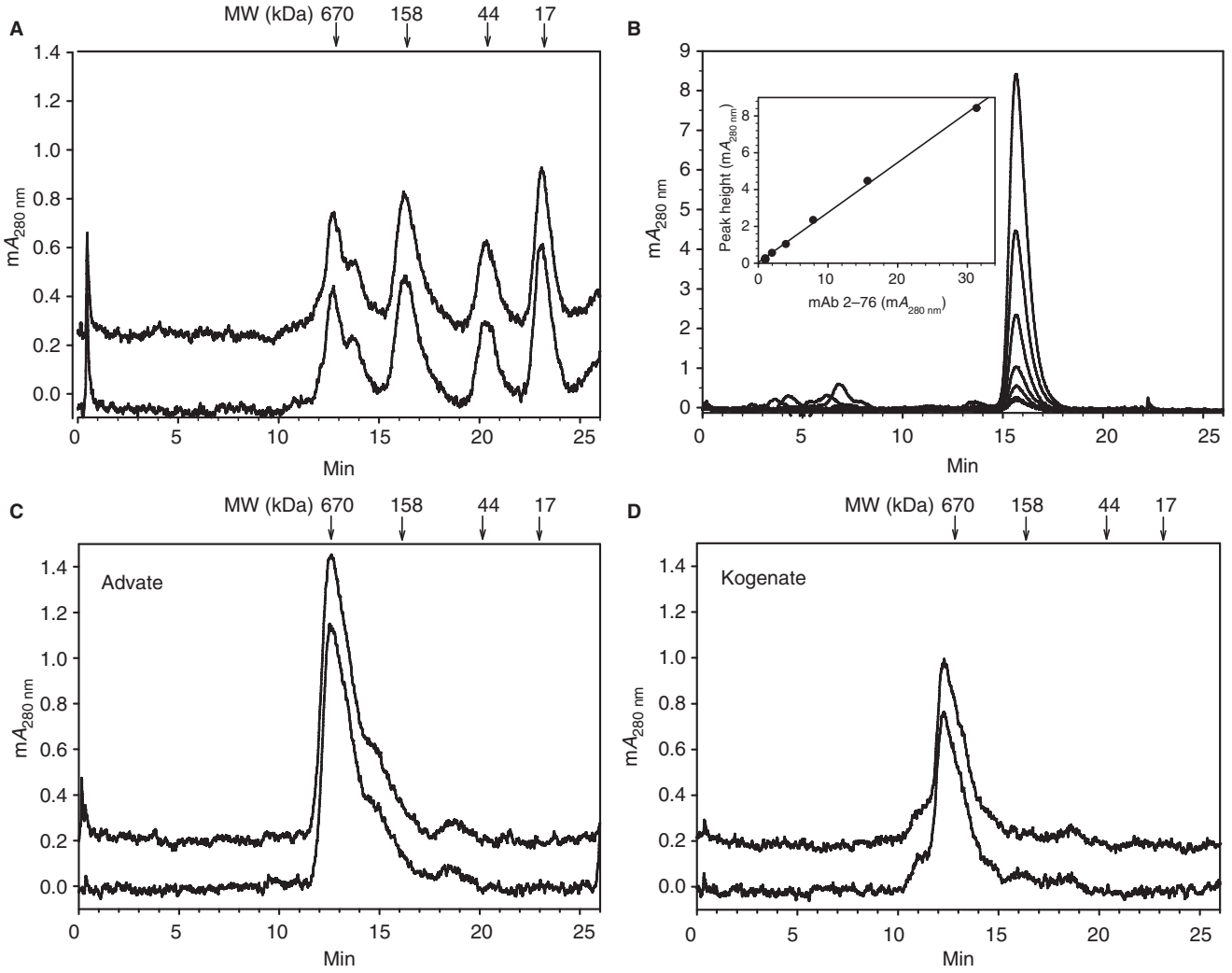

Fig. 5. Size-exclusion chromatography (SEC) of Advate and Kogenate. Molecular weight (MW) standards (A) and dilutions of mAb 2-76 (B), Advate (C) and Kogenate (D) were subjected to SEC with a Superdex 200 Increase 10/300 column as described in Materials and methods. Bio-Rad (Hercules, CA, USA) SEC standards bovine thyroglobulin (670 kDa), bovine γ-globulin (158 kDa), chicken ovalbumin (44 kDa) and horse myoglobin (17 kDa), and murine anti-human FVIII IgG m(Ab) 2-76 [64], were used for comparison. An extinction coefficient of 1.37 mg mL^{-1} cm^{-1} was used for mAb 2-76. The injection loads of Advate and Kogenate were 10.2 m$A_{280\ nm}$ and 5.6 m$A_{280\ nm}$, respectively. mAb 2-76 injection loads were 0.71, 1.4, 2.9, 5.7, 11.4 and 22.9 μg, corresponding to m$A_{280\ nm}$ values of 1, 1.9, 4.0, 7.8, 15.6, and 31.4. The chromatograms in (A), (B) and (D) represent duplicate injections with a baseline offset.

probably an aggregate consisting of a dimer of FVIII heterodimers. A bivalent dimer of FVIII heterodimers could conceivably cross-link the B-cell receptor and contribute to product immunogenicity. The 5.0–5.1 S species in Fig. 5B, D is most likely free FVIII LC, based on an $s_{20,w}$ value of 4.9 S observed for the porcine FVIII LC [26].

The major species in full-length FVIII products has an $s_{20,w}$ value of 7.4–7.5 S (Fig. 5B,D) and an estimated molecular weight of 220–230 kDa (Table 1). Therapeutic full-length FVIII is defined as the product derived from expression of the complete FVIII cDNA, which encodes a 2332-residue, 265-kDa mature polypeptide chain [60]. During intracellular processing in the mammalian cell lines used to manufacture FVIII, proteolytic cleavage occurs at residues 817, 1115, 1313 and 1648 in the B domain, leading to loss of B domain mass and expression of a paucidisperse population of heterodimers [32]. Estimates of the mole fractions of the heterodimeric species and the extent of N-linked glycosylation yielded a weight-average molecular weight of 246 kDa (Table 2), which is reasonably consistent with the experimental value.

Prior to the current study, recombinant FVIII products were considered to be highly purified preparations composed of populations of HC–LC heterodimers in which aggregates have not been described [32]. Our results provide an example of the use of SV AUC continuous $c(s)$ distribution analysis as a powerful method with which to detect aggregates in highly purified biopharmaceutical products. SEC has been the industry standard for detecting and characterizing aggregates in biopharmaceutical

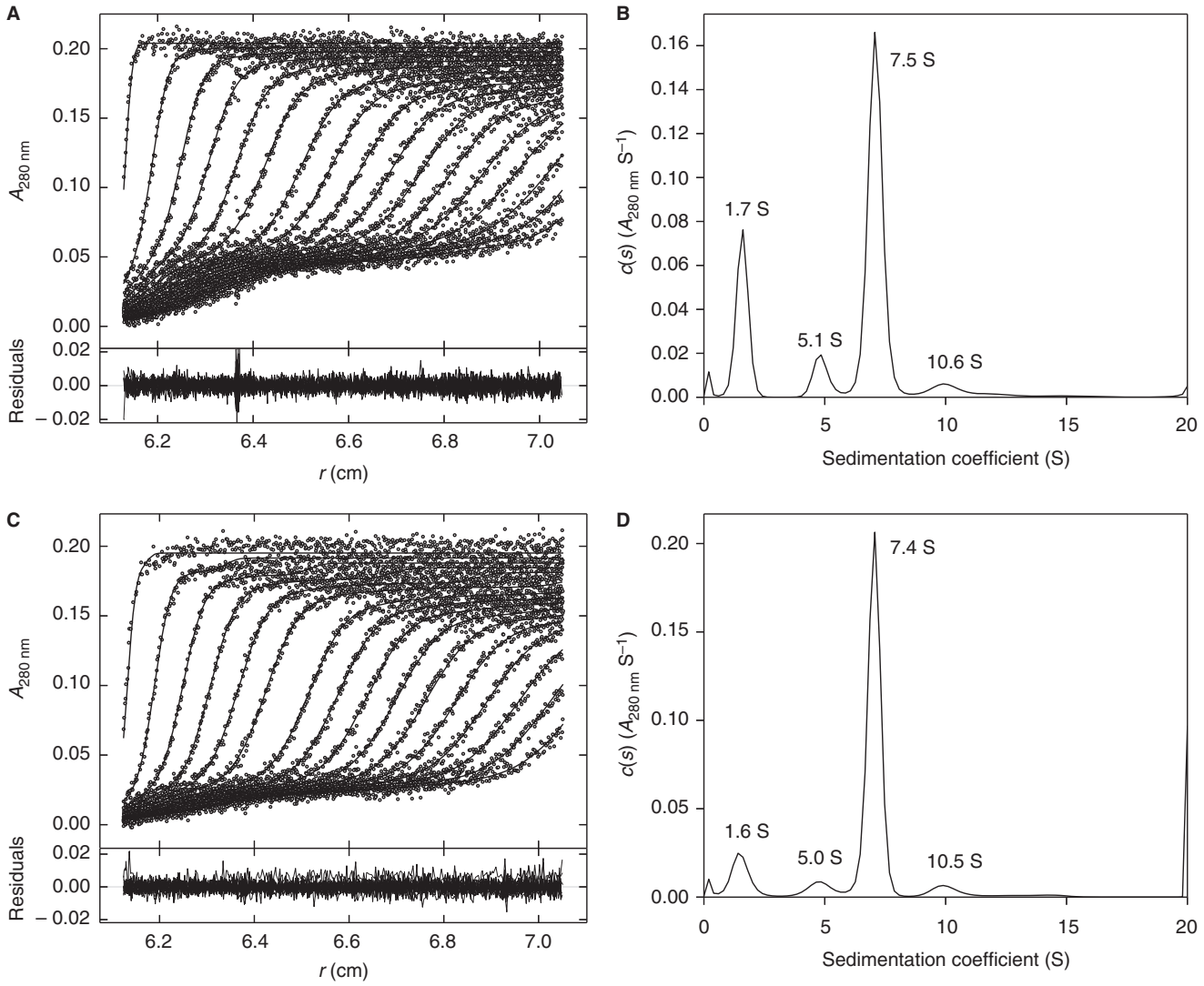

Fig. 6. Sedimentation velocity (SV) analytical ultracentrifugation (AUC) of buffer-exchanged and concentrated Advate and Kogenate. Advate (Lot 1) (A, B) and Kogenate (Lot 1) (C, D) were concentrated and exchanged into 0.15 M NaCl, 0.02 M HEPES and 5 mM $CaCl_2$ (pH 7.4) by repeated ultrafiltration, and subjected to SV AUC at 105 000 × *g* at 20 °C. (A, C) $A_{280\ nm}$ scans were taken at approximately 3-min intervals, and fitted to a continuous *c*(*s*) distribution from 0 S to 20 S with 0.2 S increments. Only every fourth scan is shown for clarity. The root-mean-square deviations of the fits are 0.0034 and 0.0032, respectively. The lower panels show residuals of the fitted data. (B, D) *c*(*s*) distributions and corresponding $s_{20,w}$ values.

Table 1 Sedimentation parameters of the major species in Advate and Kogenate

	$s_{20,w}$ (S)	f/f_0	Molecular weight (kDa)
Advate	7.5	1.82	220
Kogenate	7.4	1.91	230

products. Potential drawbacks of the use of SEC include interactions of the protein with the sieving matrix, and the requirement for a mobile phase that differs from the formulation buffer. Head-to-head comparisons of SEC with SV AUC continuous *c*(*s*) distribution analysis have demonstrated that the latter is more sensitive and identifies more species of aggregates than SEC [61,62]. Additionally, SEC requires the use of standards to estimate molecular weights, which may be inaccurate for proteins with large frictional ratios. Consistent with these observations, SEC failed to identify aggregates in Advate and Kogenate, and produced spuriously high apparent molecular weights (Fig. 5). In contrast, SV AUC provides direct information about the size and shape of molecules in paucidisperse systems. Therefore, SV AUC could be a useful additional tool for characterizing FVIII products in the biopharmaceutical industry.

In contrast to highly purified recombinant FVIII products, most of the protein mass in commercial plasma-derived FVIII/VWF products is VWF and contaminating plasma proteins. The ratio of VWF to FVIII in plasma-derived FVIII products ranges from 0.5 IU IU^{-1} to

Table 2 Weight-average molecular weight and partial specific volume of full-length recombinant factor VIII

FVIII heterodimer	Mole fraction, f_i	Molecular weight (kDa)		% Glycan (w/w)	$\bar{\nu}$ (mL g^{-1})
		Polypeptide	Glycoprotein		
HC_{1-817}–LC	0.16	173	187	7.8	0.725
HC_{1-1115}–LC	0.44	205	237	13.4	0.719
HC_{1-1313}–LC	0.40	227	271	16.2	0.716
Weight average			246		0.719

HC, heavy chain; LC, light chain.

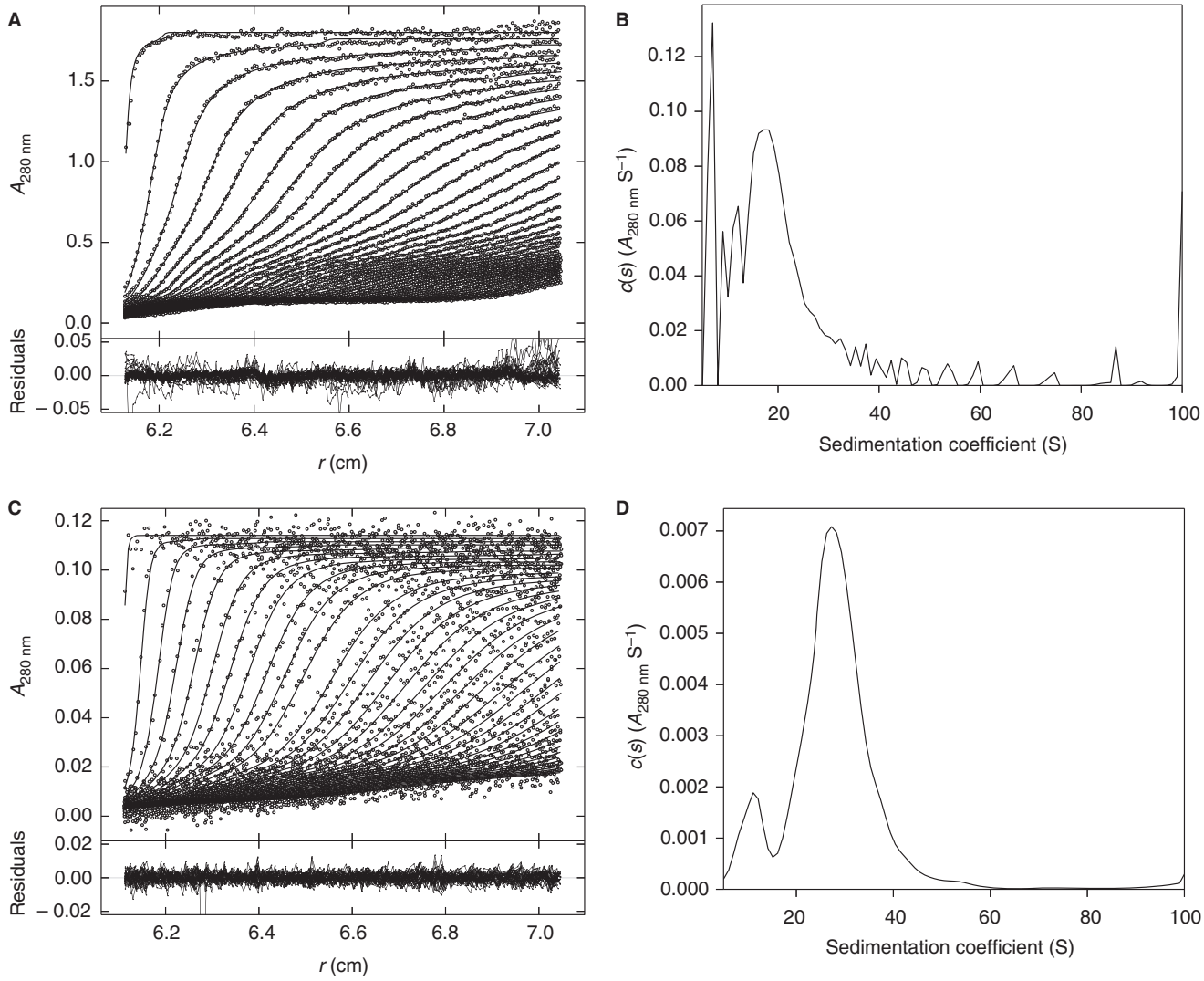

Fig. 7. Sedimentation velocity (SV) analytical ultracentrifugation (AUC) of Wilate and purified human von Willebrand factor (VWF). Wilate (A, B) was reconstituted in Sterile Water for Injection to its therapeutic formulation, and subjected to SV AUC at 105 000 × *g* at 20 °C. Human VWF (C, D) in 0.3 M NaCl and 0.2 M HEPES (pH 7.4) was subjected to SV AUC at 42 000 × *g* at 20 °C. (A, C) $A_{280\ nm}$ scans were fitted to a continuous *c*(*s*) distribution from 0 S to 100 S with 1 S increments. Only every other scan and every other data point are shown for clarity. The lower panels show the residuals of the fitted data. (B, D) *c*(*s*) distributions.

1 IU IU^{-1} [14], where 1 IU corresponds to the activity in 1 mL of normal plasma. Because the plasma concentrations of VWF and FVIII are approximately 3 μg mL^{-1} and 0.2 μg mL^{-1}, respectively, a ratio of 1 IU IU^{-1} represents a VWF/FVIII mass ratio of ≈ 15 (3/0.2). SV AUC of a commercial plasma-derived FVIII/VWF product, Wilate, and highly purified plasma-derived human VWF revealed a broad *c*(*s*) distribution, as expected, because VWF consists of a heterogeneous population of multimers. These multimers extend up to at least 20 MDa [63],

and produce a weight-average sedimentation coefficient of 30 S in highly purified preparations of plasma-derived human VWF [26]. The presence of native VWF multimers and contaminating plasma proteins confounds the use of $c(s)$ distribution analysis to detect antigen (FVIII)-specific aggregates.

Addendum

J. F. Healey performed experiments, analyzed data, and co-wrote the paper. E. T. Parker performed experiments, analyzed data, and co-wrote the paper. P. Lollar performed experiments, analyzed data, and co-wrote the paper.

Acknowledgements

Grant support: National Institutes of Health grants U54 HL112309 and Hemophilia of Georgia, Inc. (P. Lollar).

Disclosure of Conflict of Interests

P. Lollar is an inventor on patents owned by Emory University claiming compositions of matter that include modified FVIII proteins with reduced reactivity with anti-FVIII antibodies. The other authors state that they have no conflict of interest.

Supporting Information

Additional Supporting Information may be found in the online version of this article:

Table S1. Recombinant full-length FVIII products.
Table S2. Excipients and stabilizers in Product Prescribing Information.
Fig. S1. SDS-PAGE of Advate, Helixate FS, and Kogenate FS.
Fig. S2. UV absorbance spectrum of polysorbate 80.
Fig. S3. SV AUC of heat-treated Advate and Kogenate FS.

References

1 Lusher JM, Arkin S, Abildgaard CF, Schwartz RS. Recombinant factor VIII for the treatment of previously untreated patients with hemophilia A. Safety, efficacy, and the development of inhibitors. *N Engl J Med* 1993; **328**: 453–9.
2 Lusher JM, Lee CA, Kessler CM, Bedrosian CL. The safety and efficacy of B-domain deleted recombinant factor VIII concentrate in patients with severe haemophilia A. *Haemophilia* 2003; **9**: 38–49.
3 Gouw SC, van der Bom JG, Ljung R, Escuriola C, Cid AR, Claeyssens-Donadel S, van Geet C, Kenet G, Makipernaa A, Molinari AC, Muntean W, Kobelt R, Rivard G, Santagostino E, Thomas A, van den Berg HM. Factor VIII products and inhibitor development in severe hemophilia A. *N Engl J Med* 2013; **368**: 231–9.
4 Gouw SC, van den Berg HM, Fischer K, Auerswald G, Carcao M, Chalmers E, Chambost H, Kurnik K, Liesner R, Petrini P, Platokouki H, Altisent C, Oldenburg J, Nolan B, Garrido RP, Mancuso ME, Rafowicz A, Williams M, Clausen N, Middelburg RA, *et al*. Intensity of factor VIII treatment and inhibitor development in children with severe hemophilia A: the RODIN study. *Blood* 2013; **121**: 4046–55.
5 Bardi E, Astermark J. Genetic risk factors for inhibitors in haemophilia A. *Eur J Haematol* 2015; **94**(Suppl. 77): 7–10.
6 Alvarez T, Soto I, Astermark J. Non-genetic risk factors and their influence on the management of patients in the clinic. *Eur J Haematol* 2015; **94**(Suppl. 77): 2–6.
7 Wight J, Paisley S. The epidemiology of inhibitors in haemophilia A: a systematic review. *Haemophilia* 2003; **9**: 418–35.
8 Goudemand J, Rothschild C, Demiguel V, Vinciguerrat C, Lambert T, Chambost H, Borel-Derlon A, Claeyssens S, Laurian Y, Calvez T. Influence of the type of factor VIII concentrate on the incidence of factor VIII inhibitors in previously untreated patients with severe hemophilia A. *Blood* 2006; **107**: 46–51.
9 Calvez T, Chambost H, d'Oiron R, Dalibard V, Demiguel V, Doncarli A, Gruel Y, Huguenin Y, Lutz P, Rothschild C, Vinciguerra C, Goudemand J. Analyses of the FranceCoag cohort support immunogenicity differences among one plasma-derived and two recombinant factor VIII brands in boys with severe hemophilia A. *Haematologica* 2017; [epub ahead of print]. http://doi:10.3324/haematol.2017.174706.
10 Iorio A, Halimeh S, Holzhauer S, Goldenberg N, Marchesini E, Marcucci M, Young G, Bidlingmaier C, Brandao LR, Ettingshausen CE, Gringeri A, Kenet G, Knofler R, Kreuz W, Kurnik K, Manner D, Santagostino E, Mannucci PM, Nowak-Gottl U. Rate of inhibitor development in previously untreated hemophilia A patients treated with plasma-derived or recombinant factor VIII concentrates: a systematic review. *J Thromb Haemost* 2010; **8**: 1256–65.
11 Franchini M, Tagliaferri A, Mengoli C, Cruciani M. Cumulative inhibitor incidence in previously untreated patients with severe hemophilia A treated with plasma-derived versus recombinant factor VIII concentrates: a critical systematic review. *Crit Rev Oncol Hematol* 2012; **81**: 82–93.
12 Franchini M, Coppola A, Rocino A, Santagostino E, Tagliaferri A, Zanon E, Morfini M. Systematic review of the role of FVIII concentrates in inhibitor development in previously untreated patients with severe hemophilia A: a 2013 update. *Semin Thromb Hemost* 2013; **39**: 752–66.
13 Marcucci M, Mancuso ME, Santagostino E, Kenet G, Elalfy M, Holzhauer S, Bidlingmaier C, Escuriola-Ettingshausen C, Iorio A, Nowak-Gottl U. Type and intensity of FVIII exposure on inhibitor development in PUPs with haemophilia A. A patient-level meta-analysis. *Thromb Haemost* 2015; **113**: 958–67.
14 Peyvandi F, Mannucci PM, Garagiola I, El-Beshlawy A, Elalfy M, Ramanan V, Eshghi P, Hanagavadi S, Varadarajan R, Karimi M, Manglani MV, Ross C, Young G, Seth T, Apte S, Nayak DM, Santagostino E, Mancuso ME, Sandoval-Gonzalez A, Mahlangu JN, *et al*. A randomized trial of factor VIII and neutralizing antibodies in hemophilia A. *N Engl J Med* 2016; **374**: 2054–64.
15 Rosendaal FR, Palla R, Garagiola I, Mannucci PM, Peyvandi F. Genetic risk stratification to reduce inhibitor development in the early treatment of hemophilia A: a SIPPET analysis. *Blood* 2017; **130**: 1757–9.
16 Collins PW, Palmer BP, Chalmers EA, Hart DP, Liesner R, Rangarajan S, Talks K, Williams M, Hay CR. Factor VIII brand and the incidence of factor VIII inhibitors in previously untreated UK children with severe hemophilia A, 2000–2011. *Blood* 2014; **124**: 3389–97.
17 Calvez T, Chambost H, Claeyssens-Donadel S, d'Oiron R, Goulet V, Guillet B, Heritier V, Milien V, Rothschild C, Roussel-

Robert V, Vinciguerra C, Goudemand J. Recombinant factor VIII products and inhibitor development in previously untreated boys with severe hemophilia A. *Blood* 2014; **124**: 3398–408.
18 Kessler CM, Iorio A. The Rodin (Research Of Determinants of INhibitor Development among PUPs with haemophilia) study: the clinical conundrum from the perspective of haemophilia treaters. *Haemophilia* 2013; **19**: 351–4.
19 Franchini M, Mengoli C. RODIN and the pitfalls of observational studies. *Haemophilia* 2013; **19**: e315–6.
20 van der Bom JG, Gouw SC, Rosendaal FR. Second-generation recombinant factor VIII and inhibitor risk: interpretation of RODIN study findings and implications for patients with haemophilia A. *Haemophilia* 2014; **20**: e171–4.
21 Roberts CJ. Therapeutic protein aggregation: mechanisms, design, and control. *Trends Biotechnol* 2014; **32**: 372–80.
22 Gabrielson JP, Arthur KK. Measuring low levels of protein aggregation by sedimentation velocity. *Methods (Duluth)* 2011; **54**: 83–91.
23 Dam J, Schuck P. Calculating sedimentation coefficient distributions by direct modeling of sedimentation velocity concentration profiles. *Methods Enzymol* 2004; **384**: 185–212.
24 Schuck P. *Sedimentation Velocity Analytical Ultracentrifugation*. Boca Raton: CRC Press, 2017.
25 Doering CB, Parker ET, Healey JF, Craddock HN, Barrow RT, Lollar P. Expression and characterization of recombinant murine factor VIII. *Thromb Haemost* 2002; **88**: 450–8.
26 Lollar P, Hill-Eubanks DC, Parker CG. Association of the factor VIII light chain with von Willebrand factor. *J Biol Chem* 1988; **263**: 10451–5.
27 Schuck P. Size-distribution analysis of macromolecules by sedimentation velocity ultracentrifugation and Lamm equation modeling. *Biophys J* 2000; **78**: 1606–19.
28 Schuck P, Zhao H, Brautigam CA, Ghirlando R. *Basic Principles of Analytical Ultracentrifugation*. Boca Raton, FL: CRC Press, 2016.
29 Svedberg T, Pedersen KO. *The Ultracentrifuge*. New York: Oxford at the Clarendon Press, 1940.
30 Cole JL, Lary JW, Moody TP, Laue TM. Analytical ultracentrifugation: sedimentation velocity and sedimentation equilibrium. *Methods Cell Biol* 2008; **84**: 143–79.
31 Brautigam CA. Calculations and publication-quality illustrations for analytical ultracentrifugation data. *Methods Enzymol* 2015; **562**: 109–33.
32 Jankowski MA, Patel H, Rouse JC, Marzilli LA, Weston SB, Sharpe PJ. Defining 'full-length' recombinant factor VIII: a comparative structural analysis. *Haemophilia* 2007; **13**: 30–7.
33 Pace CN, Vajdos F, Fee L, Grimsley G, Gray T. How to measure and predict the molar absorption coefficient of a protein. *Protein Sci* 1995; **4**: 2411–23.
34 Medzihradszky KF, Besman MJ, Burlingame AL. Structural characterization of site-specific N-glycosylation of recombinant human factor VIII by reversed-phase high-performance liquid chromatography-electrospray ionization mass spectrometry. *Anal Chem* 1997; **69**: 3986–94.
35 Kumar HP, Hague C, Haley T, Starr CM, Besman MJ, Lundblad RL, Baker D. Elucidation of N-linked oligosaccharide structures of recombinant human factor VIII using fluorophore-assisted carbohydrate electrophoresis. *Biotechnol Appl Biochem* 1996; **24**: 207–16.
36 Shire SJ. Determination of the molecular weight of glycoproteins by analytical ultracentrifugation. *Beckman Tech Information* 1992; **DS-837**: 1–4.
37 Wuelfing WP, Kosuda K, Templeton AC, Harman A, Mowery MD, Reed RA. Polysorbate 80 UV/vis spectral and chromatographic characteristics – defining boundary conditions for use of the surfactant in dissolution analysis. *J Pharm Biomed Anal* 2006; **41**: 774–82.
38 Miller CH, Platt SJ, Rice AS, Kelly F, Soucie JM. Hemophilia Inhibitor Res Study I. Validation of Nijmegen-Bethesda assay modifications to allow inhibitor measurement during replacement therapy and facilitate inhibitor surveillance. *J Thromb Haemost* 2012; **10**: 1055–61.
39 Schuck P, Rossmanith P. Determination of the sedimentation coefficient distribution by least-squares boundary modeling. *Biopolymers* 2000; **54**: 328–41.
40 Braun AC, Ilko D, Merget B, Gieseler H, Germershaus O, Holzgrabe U, Meinel L. Predicting critical micelle concentration and micelle molecular weight of polysorbate 80 using compendial methods. *Eur J Pharm Biopharm* 2015; **94**: 559–68.
41 Rosenberg AS. Effects of protein aggregates: an immunologic perspective. *AAPS J* 2006; **8**: E501–7.
42 Guidance for Industry. *Immunogenicity Assessment for Therapeutic Protein Products Office of Communications*: Division of Drug Information, Center for Drug Evaluation and Research, Food and Drug Administration, US Department of Health and Human Services, 2014. https://www.fda.gov/downloads/drugs/guidances/ucm338856.pdf.
43 Gamble CN. The role of soluble aggregates in the primary immune response of mice to human gamma globulin. *Int Arch Allergy Appl Immunol* 1966; **30**: 446–55.
44 Ellis EF, Henney CS. Adverse reactions following administration of human gamma globulin. *J Allergy* 1969; **43**: 45–54.
45 Moore WV, Leppert P. Role of aggregated human growth hormone (hGH) in development of antibodies to hGH. *J Clin Endocrinol Metab* 1980; **51**: 691–7.
46 Ryff JC. Clinical investigation of the immunogenicity of interferon-alpha 2a. *J Interferon Cytokine Res* 1997; **17**(Suppl. 1): S29–33.
47 Josic D, Buchacher A, Kannicht C, Lim YP, Loster K, Pock K, Robinson S, Schwinn H, Stadler M. Degradation products of factor VIII which can lead to increased immunogenicity. *Vox Sang* 1999; **77**(Suppl. 1): 90–9.
48 Srinivas Reddy A, Tsourkas PK, Raychaudhuri S. Monte Carlo study of B-cell receptor clustering mediated by antigen crosslinking and directed transport. *Cell Mol Immunol* 2011; **8**: 255–64.
49 Sauerborn M, Brinks V, Jiskoot W, Schellekens H. Immunological mechanism underlying the immune response to recombinant human protein therapeutics. *Trends Pharmacol Sci* 2010; **31**: 53–9.
50 Seong SY, Matzinger P. Hydrophobicity: an ancient damage-associated molecular pattern that initiates innate immune responses. *Nat Rev* 2004; **4**: 469–78.
51 Sharma B. Immunogenicity of therapeutic proteins. Part 1: Impact of product handling. *Biotechnol Adv* 2007; **25**: 310–17.
52 Dintzis RZ, Okajima M, Middleton MH, Greene G, Dintzis HM. The immunogenicity of soluble haptenated polymers is determined by molecular mass and hapten valence. *J Immunol* 1989; **143**: 1239–44.
53 Bachmann MF, Rohrer UH, Kundig TM, Burki K, Hengartner H, Zinkernagel RM. The influence of antigen organization on B cell responsiveness. *Science* 1993; **262**: 1448–51.
54 Joubert MK, Hokom M, Eakin C, Zhou L, Deshpande M, Baker MP, Goletz TJ, Kerwin BA, Chirmule N, Narhi LO, Jawa V. Highly aggregated antibody therapeutics can enhance the *in vitro* innate and late-stage T-cell immune responses. *J Biol Chem* 2012; **287**: 25266–79.
55 Arakawa T, Timasheff SN. Stabilization of protein structure by sugars. *Biochemistry* 1982; **21**: 6536–44.
56 Xie G, Timasheff SN. The thermodynamic mechanism of protein stabilization by trehalose. *Biophys Chem* 1997; **64**: 25–43.

57 Lee JC, Timasheff SN. The stabilization of proteins by sucrose. *J Biol Chem* 1981; **256**: 7193–201.
58 Ebel C, Eisenberg H, Ghirlando R. Probing protein–sugar interactions. *Biophys J* 2000; **78**: 385–93.
59 Cantor CR, Schimmel PR. *Ultracentrifugation. Biophysical Chemistry Part II Techniques for the Study of Biological Structure and Function*. San Francisco: W. H. Freeman and Co., 1980: 591–642.
60 Vehar GA, Keyt B, Eaton D, Rodriguez H, O'Brien DP, Rotblat F, Oppermann H, Keck R, Wood WI, Harkins RN, Tuddenham EGD, Lawn RM, Capon DJ. Structure of human factor VIII. *Nature* 1984; **312**: 337–42.
61 Gabrielson JP, Brader ML, Pekar AH, Mathis KB, Winter G, Carpenter JF, Randolph TW. Quantitation of aggregate levels in a recombinant humanized monoclonal antibody formulation by size-exclusion chromatography, asymmetrical flow field flow fractionation, and sedimentation velocity. *J Pharm Sci* 2007; **96**: 268–79.
62 Gabrielson JP, Arthur KK, Stoner MR, Winn BC, Kendrick BS, Razinkov V, Svitel J, Jiang Y, Voelker PJ, Fernandes CA, Ridgeway R. Precision of protein aggregation measurements by sedimentation velocity analytical ultracentrifugation in biopharmaceutical applications. *Anal Biochem* 2010; **396**: 231–41.
63 Sadler JE. Biochemistry and genetics of von Willebrand factor. *Annu Rev Biochem* 1998; **67**: 395–424.
64 Healey JF, Parker ET, Barrow RT, Langley TJ, Church WR, Lollar P. The humoral response to human factor VIII in hemophilia A mice. *J Thromb Haemost* 2007; **5**: 512–7.